Patterns of morphological variation highlight the effect of natural selection on eyespots modularity in the butterfly Morpho telemachus

Ariane Chotard, Violaine Llaurens, Vincent Debat

Title: Patterns of morphological variation highlight the effect of natural selection on eyespots modularity in the butterfly *Morpho telemachus*

Ariane Chotard, Violaine Llaurens, Vincent Debat
Institut de Systématique, Evolution, Biodiversité (ISYEB), Muséum National d'Histoire Naturelle, CNRS, Sorbonne Université, EPHE, Paris, France
45 rue Buffon, CP50, 75005, Paris, France.
Email: ariane.chotard@gmail.com

Abstract (200/200):
Morphological correlations can stem from developmental constraints but also from selective pressures. Butterfly eyespots are repeated wing color pattern elements, widespread across species. As developmental serial homologues, they are controlled by similar developmental pathways imposing correlations among eyespots: selection on a single eyespot may induce correlated responses in all eyespots. We study the variations in the ventral eyespots of *Morpho telemachus*, where two different selective regimes are likely to act: while most eyespots are always-visible, two eyespots are conditionally-displayed: hidden at rest, they can be exposed when the butterflies are threatened, or during sexual interactions. We investigate how such contrasted selection across eyespots can alter the covariations imposed by their shared developmental origin. We quantified eyespots co-variations within a large population of *M. telemachus* and compared the observed patterns to those found in *M. helenor*, where all eyespots are always-visible and thus probably affected by a similar selection regime. We found that *M. telemachus* conditionally-displayed eyespots are less variable than always-visible eyespots and that these two eyespots form a separate variational module in this species, in contrast to *M. helenor*. Our results suggest that eyespots covariations were shaped by selection, highlighting how natural selection may promote the evolution of modularity.

Keywords: Stabilizing selection, developmental constraints, variation, modularity, butterflies, fluctuating asymmetry

Introduction

The level of evolutionary constraints on any morphological trait depends on its correlations with other traits, that originate from genetic, developmental and physical connections among traits. Ancestral correlations can strongly influence the evolution of traits under selection. For example, adaptive radiations have been suggested to occur primarily along the lines of least resistance, drawn by constraining effects of genetic correlations (Schluter 1996). But the correlations among traits can also evolve in response to selection: for example, deleterious pleiotropic effects can be eliminated or compensated for (e.g. Pavlicev and Wagner 2012), and correlational selection (joint selection of several traits) can favor certain genetic correlations (e.g. Sinervo and Svensson 2002). Correlations among traits – trait integration – but also their independence from other traits – trait modularity – thus stem from both selective and developmental factors (e.g. Wagner 1996; Klingenberg, 2008). Whether the patterns of modularity mostly reflect the developmental constrains exerted on the evolution of traits or the selection regime is a long-standing question (e.g. Cheverud, 1984; Kirschner and Gerhard 1998; Schlosser and Wagner, 2005; Wagner et al. 2007; Klingenberg 2008; Mello et al. 2016).

Serial homologues, like vertebrate teeth (Van Valen 1994) or arthropod segments (Emerson & Schram 1990), are relevant traits to identify how selection can act on morphological integration. Such homologous traits stem from the repetition of the same developmental pathway in different locations of the body (Hall 1995). Serial homologues are thus expected to present a tight covariation due to their shared developmental basis (Young and Hallgrimsson 2005). In contrast, heterogeneous selection across the elements of a series might drive their divergence and break down their co-variation (Wagner and Altenberg 1996; Melo and Marroig, 2015). The patterns of covariation across serial homologues therefore reflect the prevailing effect of developmental *vs*. selective factors affecting trait evolution (Beldade and Brakefield, 2003; Allen 2008): a tight covariation across serial homologues would indicate a prominent effect of shared developmental pathways, while a modular structuration of the series, opposing co-selected elements to others, would rather suggest a prominent role of selection.

Butterfly eyespots are a textbook example of serial homology: these circular color patterns are repeated across the wings in many butterfly species. All eyespots are formed by the expression of a common developmental cascade at different locations on the wings, as shown by developmental studies carried out in the model species *Bicyclus anynana* (see Monteiro 2015 for a review). Such serial developmental homology results in strong genetic correlations across eyespots: artificial selection on a particular eyespot indeed induces a correlated response on all

eyespots, consistent with their developmental integration (Monteiro *et al.* 1994, 1997; Beldade *et al.* 2002; Beldade & Brakefield 2002, 2003).

The wide diversity of eyespot morphology – including size, shape, and color – suggests that diverse selective pressures affect their evolution (Kodandaramaiah 2011). In some species, eyespots are conditionally-displayed: hidden at rest, they can be uncovered at will. Usually large and highly conspicuous, these eyespots might intimidate predators if suddenly uncovered during an attack (Stevens 2005; Dapporto *et al.* 2019). Radically different eyespots observed in other species, with a small size and peripheral location, are constantly visible at rest. Such eyespots might divert predator attacks away from the vital parts of the body (Lyytinen *et al.* 2004; Stevens 2005; Olofsson *et al.* 2010 ; Prudic *et al.* 2015). The continuum of ecological contexts encountered by different butterfly species may explain the important variations in eyespots across species (Kodandaramaiah 2011). On top of selection by predators, sexual selection might also affect eyespot evolution. In *B. anynana*, UV reflectance in the center of the ventral conditionally-displayed eyespot, affects males mate choice (Huq *et al.* 2019), promoting UV coloration in these particular eyespots. The heterogeneous morphology of eyespots from the same series observed within many butterfly species suggests that contrasted selective pressures may affect them, potentially breaking their covariation and leading to their morphological divergence.

Here we investigate how contrasted selective pressures may disrupt developmental constraints, by assessing morphological covariations across eyespots within the butterfly species *Morpho telemachus* (Linné, 1758), where the different eyespots are likely submitted to different selective regimes. In the *Morpho* genus, a series of eyespots is observed on the ventral side of the wings (Debat *et al.* 2020), exposed when the butterflies are resting. In contrast with most *Morpho* species, *M. telemachus* has two large conditionally-displayed eyespots on the ventral side of the forewing (Figure 1) that are usually hidden at rest by the overlapping hindwing but can be revealed when the butterfly spreads its wings. These eyespots might have an intimidating effect on predators if unmasked during an attack, as suggested in other butterfly species (Stevens 2005; Dapporto *et al.* 2019): paired eyespots are indeed particularly intimidating (Stevens 2005; Inglis *et al.* 2010). They could also be part of a concealable sexual signal. The remaining eyespots, located on the hindwing and on the forewing tip, are always-visible, suggesting they might be submitted to a different selective pressure, possibly contributing to the general cryptic appearance of the butterfly at rest. Such contrasted selective regimes across eyespots in *M. telemachus* provide a relevant opportunity to investigate the

impact of selection on the pattern of covariation across a series of developmental homologues. While shared developmental pathways may generate tight morphological covariations among eyespots (Brakefield, 2001; Allen, 2008), the differential selection on a subset of eyespots should promote their relative independence.

Because the covariation between different eyespots of the series might ancestrally differ, we contrasted patterns of variations observed in *M. telemachus* with another Morpho species, *Morpho helenor* (Cramer, 1776). Like in most other Morpho species, including the two species branching at the basis of Morpho phylogeny (Chazot et al. 2016; Debat *et al.* 2020), all eyespots of *M. helenor* are always-visible, suggesting that, in contrast to *M. telemachus*, similar selective pressures affect all eyespots of the series. Comparing the patterns of eyespot covariation of *M. telemachus* and *M. helenor* should thus shed light on the effect of heterogeneous selection on the evolution of eyespot modularity. In *M. helenor*, the congruent selective and developmental effects should favor the tight covariation of all eyespots, while in *M. telemachus*, a pattern of covariation opposing always-visible and conditionally-displayed eyespots should be detected, would the contrasted selective pressures prevail.

We first assessed the conspicuousness of the different eyespots in the two species, by measuring the reflectance spectra of the yellow and black rings forming the eyespots and computing the color contrast perceived by avian predators. We measured the size and shape of the two rings within each eyespot and then assessed their patterns of variations and covariations at two levels. First, we assessed variance among individuals, that reflects genetic and environmental differences among individuals. Then, we study variance within individuals, i.e. fluctuating asymmetry (FA), stemming from random developmental variation leading to subtle differences between right and left sides for a given trait (Palmer and Strobeck 1986). FA covariation across traits is then assumed to reflect developmental integration, as it is expected to result from direct developmental interactions across traits (Klingenberg 2003, 2008, 2014). To assess the impact of selection on trait evolution and modularity, we used two sets of analyses. (1) By comparing the levels of variation of the different eyespots within each species, we predicted a homogeneous variation in all eyespots in *M. helenor* as a result of a similar selection acting on all eyespots. In contrast, if different selection pressures affect the two types of eyespots in *M. telemachus*, they should present contrasted levels of variation as compared to other eyespots. (2) By comparing the covariations between traits within species, we predicted a global pattern of correlation across eyespots in *M. helenor*, resulting from homogeneous selective effects. In contrast, in *M. telemachus*, we predicted different patterns of modularity in

the conditionally-displayed *vs*. always-visible eyespots, as a result of the contrasted selective regimes.

Materials & Methods

Butterfly Samples

M. telemachus is a canopy species distributed throughout the Amazon basin, from the foothills of the Andes to the Brazilian Atlantic Forest (Blandin et Purser 2013). We focused on an exceptional sample composed of 370 males from a single emergence bloom of *M. telemachus exsusarion* (Le Moult & Réal 1962) collected in 1995 in Bolivia, in the province of Chapare (Department of Cochabamba CBBA; Gilbert Lachaume, pers. com.). This sample provides a relevant opportunity to assess eyespot variability within a natural population. All individuals likely encountered similar environmental conditions, reducing the potential effects of phenotypic plasticity.

We compared the levels of variation in the different eyespots within this population of *M. telemachus* to the variation of the same eyespots in a closely-related species, *M. helenor*. We gathered specimens of *M. helenor* from the collections of the Muséum National d'Histoire Naturelle (Paris), by sampling 31 males originating from two localities (Chapare - Bolivia/ Perene - Peru). Since these collection specimens were originally caught by different collectors at different localities, the morphological variation measured in *M. helenor* combines intra- and inter-populational differences – either genetic or environmental – and thus likely over-estimates phenotypic variation.

Estimating eyespot conspicuousness

To estimate the level of conspicuousness of the different eyespots, we measured their color contrast on a subsample of 10 individuals per species. For each eyespot, the reflectance spectrum of the yellow and the black ring was measured using a spectrophotometer (AvaSpec-ULS2048CL-EVO-RS, software AvaSoft v.8.12.0.0), sensitive to wavelengths between 200 and 1100 nm. A light source (Avalight-DH-S-BAL) covering the visible and UV wavelengths from 300 to 700 nm was used to illuminate the specimens (coupling a deuterium lamp with a spectrum of 215 to 500 nm, and a halogen lamp from 500 to 2500 nm). Our measurements were conducted while minimizing external light sources. To assess the contrast between the two rings as perceived by avian predators, we quantified chromatic and achromatic contrasts (Olsson *et*

al. 2018) using the two major visual systems documented in birds (UV and violet-sensitive respectively), as implemented in the R package PAVO2 (Maia *et al.* 2019). The vision models were all applied with standard conditions (Weber fraction value of 0.05 - Dell'Aglio *et al.* 2018) with the following relative cone densities 0.37:0.7:0.99:1 for UV-sensitive model (UVS:S:M:L) and 0.25:0.5:1:1 for Violet-sensitive model (VS:S:M:L) (Finkbeiner *et al.* 2017). The chromatic and achromatic contrast analyses were performed using a bootstrap procedure. Contrasts are expressed in JND (*Just Noticeable Difference*) with a threshold of 1 JND. Values above that threshold will be considered as noticeable by an avian observer.

Measuring eyespot size and shape: Imaging and morphometric measurements

The four wings of each individual were photographed in a photo studio under controlled LED light using a Nikon D90 (Camera lens: AF-S Micro Nikkor 60 mm 1:2.8G ED), in standardized conditions allowing to minimize shape distortion due parallax. Each eyespot is composed of two concentric rings: an external yellow ring and an internal black ring, around a central white pupil. *M. telemachus* usually has 9 ventral eyespots (Figure 1A-B): 4 on the forewing and 5 on the hindwing. Nevertheless, two of these eyespots (E2 and E6 - visible on Figure 1B) were very often extremely reduced or absent; in addition, these eyespots are never found in *M. helenor* (Figure 1B). We thus excluded them from our protocol and focused on the 7 eyespots observed on all specimens.

For both species, length and width of the yellow and black rings (respectively noted L_y, W_y and L_b, W_b, Figure 1C) were measured on all eyespots using ImageJ (version 1.8.0_112). Following previous studies (Monteiro *et al.* 1997; Breuker *et al.* 2007; Allen 2008), length was measured along the direction parallel to the veins framing the eyespot and passing through the center of the eyespot and width along the perpendicular to that direction (Figure 1C). To characterize the shape of the different eyespots, we computed the ratio between length and width of the two rings for each eyespot ($R_y=L_y/W_y$ and $R_b=L_b/W_b$) and used $(1 – R)$ as a measure of their departure from perfect circularity. All measurements were made on both left and right eyespots, to assess asymmetry.

Assessing patterns of variations and covariations

Estimating fluctuating asymmetry

Fluctuating asymmetry (FA) is the deviation from perfect bilateral symmetry due to developmental noise, *i.e.* the small, random variation independently affecting the two sides of

a trait during development (Palmer and Strobeck, 1986). FA was measured as the variance of the right minus left values distribution (FA4 in the terminology of Palmer 1994). To avoid measurement bias due to the lateralization of the human observer, mirror images of the left wings were used (package TransformJ, Meijering *et al.* 2001), and the order of measurements (right or left) randomized.

Checking measurement error and allometric effects on FA

To quantify measurement error (ME), a random sub-sample of 30 individuals was measured 3 times, and the impact of ME on FA was assessed. We estimated ME on the different traits, using the repeated measurements protocol described in Palmer and Strobeck (1986) and Palmer (1994). We applied two-way mixed model ANOVAs with 'side' as a fixed effect and 'individual' as a random effect, for each of the 28 variables. In these models, the interaction term (side x individual) assesses FA and its statistical significance tests whether FA is greater than ME, which is included in the residual term. For all measurements, individual variation and fluctuating asymmetry were significantly larger (on average 11.6 times) than ME, suggesting that FA is not strongly affected by error.

To test whether larger eyespots display higher asymmetries, we computed the correlation of trait asymmetry values $(L-R)$ and trait average size $(L+R)/2$. As no correlation was detected ($r = -0.01$, $p = 0.284$), correction for eyespot size was not applied. In contrast, a significant positive correlation was detected between eyespot size and eyespot variance ($r = 0.79$, $p < 0.001$). Inter-individual variation of linear measurements was thus assessed by their coefficient of variation (*CV*). Finally, to assess whether larger butterflies tended to display higher asymmetries, we tested the correlation between asymmetry values and wing area, used as a proxy of butterfly size. A significant correlation was detected, but it was very low ($r = 0.026$, $p < 0.01$), suggesting that allometric effects are weak.

Comparing eyespots variability

We then estimated the levels of variation of the different traits within each of the two species. Differences in mean size (L_y, W_y, L_b and W_b) and shape (ratios R_y and R_b) among eyespots were tested using pairwise Welch tests, which allows to compare means of multiple samples with unequal variances. FA and inter-individual variances were compared across eyespots using pairwise *F*-tests, because FA was computed as a variance. Coefficients of variation of size were compared using an asymptotic test for the equality of multiple coefficients of variation (based

on the calculation of the *D'AD* statistic proposed by Feltz and Miller 1991 - R package "cvequality", Marwick and Krishnamoorthy 2019). Multiple testing was accounted for by using Holm-Bonferroni procedure. We then compared the intraspecific levels of variations of all eyespots between species using *F*-tests.

As the sample sizes were very different (370 for *M. telemachus* and 31 for *M. helenor*), the interspecific comparisons were based on a bootstrap procedure, by random subsampling 10000 batches of 31 *M. telemachus.*

Assessing the patterns of modularity across eyespots

To identify the different variational modules, we estimated morphological covariations between traits within each species. The covariation of morphological traits across individuals can stem from different factors, including environmental effects (plasticity), but also allelic variation in genes involved in the underlying developmental pathway (pleiotropy). In contrast, FA covariation (*i.e.* the covariation of trait asymmetries across individuals) results from the direct effect of shared developmental factors. Since FA is inherently random, its values can be correlated across traits only if those traits directly interact during development: this can happen when the traits are physically linked or share a part of their developmental pathways (*e.g.* common precursor, or global pre-patterning) (Klingenberg 2003, 2008; Breuker et al. 2007). We thus quantified both covariation between traits values, averaged across sides (individual covariation) and covariation between traits asymmetries (FA covariation).

We specifically compared the covariations among always-visible eyespots with those among the two conditionally-displayed eyespots of *M. telemachus*, by computing the average inter-eyespot correlations. The patterns of modularity across eyespots were estimated using correlation matrices restricted to statistically significant correlations among traits. Correlation matrices were visually displayed as networks in which each variable is a node and each correlation an edge, using the package qgraph (Epskamp *et al.* 2012). The hypotheses of modularity were then tested using a hierarchical module partition using Ward's hierarchical cluster analysis (Ward 1963; Zelditch *et al.* 2008) using the function pvclust of the pvclust package (Suzuki *et al.* 2006), which calculates *p*-values for hierarchical clustering via multiscale bootstrap resampling. Each node supported by a significant *p*-value defines a module. This method has the advantage of allowing to detect nested modularity patterns and thus, a simultaneous analysis of the intra- and inter-eyespots modularity.

All statistical analyses were carried out in R version 3.6.3 (R Core Team 2020).

Results

Contrasted levels of conspicuousness among eyespots in M. telemachus

In *M. telemachus*, conditionally-displayed eyespots were significantly larger than all other eyespots (41.46% for L_y, 37.10% for W_y, 49.03% for L_b and 37.67% for W_b, on average; Figure 2A, Table S1). Their shape was also significantly rounder than in other eyespots (Figure 2B, details in Tables S2). Achromatic contrasts in *M. telemachus* were heterogeneous across eyespots, conditionally-displayed eyespots displaying particularly high values (55.69% higher than other eyespots in UV-models and 56.81% higher in Violet-models, on average; Figure 2C). Conversely, achromatic contrasts in *M. helenor* eyespots were homogeneously high, comparable to *M. telemachus* conditionally-displayed eyespots (Figure 2C). The reduced size and achromatic contrast of the always-visible eyespots of *M. telemachus* suggest a strong decrease in conspicuousness in these eyespots as compared to the conditionally-displayed eyespots of *M. telemachus* and to all eyespots of *M. helenor*. Such difference was nevertheless not observed for chromatic contrasts (Figure S1), suggesting that similar coloration was conserved throughout all eyespots in both species.

The shape of always-visible eyespots is more variable and asymmetrical in M. telemachus

For both species, the variability of eyespot size, as estimated by the variation among individuals and by fluctuating asymmetry, was quite homogeneous across eyespots: most pairwise comparisons of size variation between eyespots were non-significant (fluctuating asymmetry see Figures S2; individual variation: L_y: $D'AD = 1.87$, $p = 0.93$; L_b: $D'AD = 0.91$, $p = 0.99$; W_y: $D'AD = 2.84$, $p = 0.83$; W_b: $D'AD = 2.36$, $p = 0.88$ - Figure S3). In contrast, variability of eyespot shape was strikingly different across eyespots in *M. telemachus*. Overall, both individual variation and asymmetry of shape were lower in the two conditionally-displayed eyespots than in the always-visible eyespots (Figure 3), and particularly strikingly so for the yellow ring (on average 4.01 times less variable and 10.08 times less asymmetric than the always-visible eyespots). Such low variability of shape in the conditionally-displayed eyespots suggests a selective effect on the roundness of these eyespots.

Overall, eyespot shape variability tended to be lower in *M. helenor* than in *M. telemachus*: among-individual variation was on average 1.62 and 2.79 times lower, in the yellow and black

rings (F_{yellow}= 1.62, df = 2566, $p < 0.001$; F_{black}= 2.80, df = 2564, $p < 0.001$ - Figure 3), and FA was 3.13 and 2.27 times lower (F_{yellow}= 3.13, df = 2566, $p < 0.001$; F_{black}= 2.27, df = 2564, $p < 0.001$ - Figure 3). This difference was particularly strong for always-visible eyespots, which were very variable between individuals in *M. telemachus*, and much more stable in *M. helenor*. Combined with a generally more conspicuous appearance of all eyespots in *M. helenor*, this stability of eyespot shape points at a similar selection regime acting on all eyespots in this species. Overall, the comparison of the two species suggests a similarly low variability in the whole series of eyespots in *M. helenor*, as well as in the conditionally-displayed eyespots in *M. telemachus*. In contrast, the always-visible eyespots of *M. telemachus* are much more variable.

Conditionally-displayed eyespots form a variational module in M. telemachus

Figure 4 clearly shows that there were more correlations across traits (individual variation) than across traits asymmetries (FA). Since covariations in FA reflect direct developmental interactions among traits, correlations are expected within physically-interacting traits, *e.g.* within each eyespot, while correlations in FA across eyespots are expected to be limited. The patterns of covariation obtained from inter-individual variation and FA matrices were nevertheless mostly congruent. Unexpectedly, the different eyespots tended to vary independently from one another, the two rings tightly covarying within an eyespot, but more loosely among eyespots. This is particularly striking in *M. helenor* for individual variation (Figures 4A and 5A; mean correlations: $cor_{within\ all\ eyespots}$ =0.94±0.05; $cor_{among\ all\ eyespots}$=0.54±0.14; see Table S3 for all correlations categories), but also for FA (Figures 4B and 5B; mean correlations: $cor_{within\ all\ eyespots}$ = 0.67±0.24; $cor_{among\ all\ eyespots}$ =0.03±0.19). Consistent with a homogeneous effect of selection on the whole series of eyespots in *M. helenor*, no sub-clustering of eyespots is detected in this species.

In contrast, in *M. telemachus*, the two conditionally-displayed eyespots exhibit strong covariations and clearly form a separate variational module. Their FA covariation is also three times higher than that of always-visible eyespots ($cor_{conditionally\text{-}displayed\ CD}$ = 0.30±0.17; $cor_{always\text{-}visible}$ = 0.11±0.12; see Table S3 for all correlations categories). Figure 5 highlights that most eyespots form distinct modules, within which the width and length of each ring (black or yellow) are correlated. In contrast, the different measurements performed on the two conditionally-displayed eyespots tightly cluster, irrespective of eyespot identity (Figure 5C). The same pattern is found for individual variation, the covariation among conditionally-displayed eyespots being even almost as high as that measured within a single eyespot

($cor_{conditionally\text{-}displayed}$ = 0.74±0.12, $cor_{always\text{-}visible}$ = 0.49±0.10 $cor_{within\ all}$= 0.82±0.18). Overall, this opposition between conditionally-displayed *vs*. always-visible eyespots suggests a change in the modularity pattern in *M. telemachus* as compared to *M. helenor*.

Discussion

Differential eyespot variability in M. telemachus shaped by contrasted selection regimes

In *M. telemachus*, the large difference in achromatic contrast detected between conditionally-displayed eyespots and the others (Figure 2C), suggests that the two types of eyespots may be submitted to different selective regimes. Achromatic contrast is indeed often used by birds to detect small targets while chromatic contrast is involved in discrimination of large targets and recognition of chromatic patterns (Osorio *et al.* 1999; Théry *et al.* 2004; Halpin *et al.* 2020). Achromatic contrast was also shown to increase prey conspicuousness and detection by mantid predators (Prudic *et al.* 2007). Our results thus highlight that conditionally-displayed eyespots are more conspicuous than the other eyespots. Their evolution might thus have been influenced by different selective pressures.

Our analyses then showed that in *M. telemachus*, conditionally-displayed eyespots are larger and rounder than the always-visible eyespots. Their shape is also strikingly less variable, with levels of variation and fluctuating asymmetry (FA) comparable to those detected in *M. helenor* (Figure 3). This is consistent with an effect of stabilizing selection, expected to reduce genetic variation (Stearns *et al.* 1995; Boonekamp *et al.* 2018). Stabilizing selection might also favor eyespot developmental robustness, reducing variation and FA via enhanced canalization and developmental stability (Schmalhausen, 1949; Palmer and Strobeck 1986; Clarke 1998; Leamy and Klingenberg 2005; Garnier *et al.* 2006; but see Pelabon *et al.* 2010).

Most Morpho species, including the species *M. eugenia* and *M. marcus*, branching at the basis of the Morpho phylogeny, display large and conspicuous eyespots similar to those of *M. helenor* (Debat *et al.* 2020). The small size and high variability of the always-visible eyespots in *M. telemachus* is thus likely a derived condition. This higher variability might be related to a relaxation of selection on these eyespots. Non-functional and vestigial structures are indeed expected to present increased morphological variance and FA (reviewed in Lahti et al. 2009), as observed in the reduced wings of some insects (e.g. carabid: Garnier *et al.* 2006; gall thrips: Crespi and Vanderkist, 1997) or the reduced digits of some mammals (in primates: Tague, 1997, 2002, or canids: Tague, 2020). We recently reported a negative correlation between eyespot

size and intraspecific variability of eyespot size and shape across the whole *Morpho* genus (Debat *et al.* 2020), suggesting that beyond the particular example of *M. telemachus*, stabilizing selection on the smallest eyespots might be relaxed compared to larger ones.

The high variability of *M. telemachus* always-visible eyespots might also be explained by other specific selective regimes, like apostatic selection (Allen and Clarke 1968; Ursprung and Nöthiger 1972 Bond 2007), a form of negative frequency-dependent selection favoring rare phenotypes in prey. Rarely encountered morphologies would be more difficult to identify by predators, as suggested for the cryptic patterns of moths (Bond and Kamil 2002, 2006). Apostatic selection may thus favor low frequency variants in *M. telemachus* always-visible eyespots, improving crypsis. While this selection in principle relies on genetic variants, it might also favor low levels of developmental robustness. The high FA measured in these eyespots raises the interesting possibility of an adaptive developmental instability (Forde 2009).

The pattern of eyespot modularity is likely shaped by selection in M. telemachus

In both species, the covariation among eyespots was markedly lower than within eyespots, for both FA and individual variation. This result was expected for FA, as direct developmental interactions across eyespots are expected to be limited to the common global pre-patterning of the wing or to physically close traits (e.g. Breuker et al. 2007). Considering individual variation, the relative independence of the different eyespots was unexpected. Eyespots serial homology indeed implies that genetic variation affecting any of the components of the shared genetic network should trigger a joint phenotypic variation. Similarly, any environmental influence on this common network should increase phenotypic covariance (*e.g.* Allen 2008). A tight covariation across eyespots was in particular predicted in *M. helenor*, where all eyespots are expected to be submitted to the same selection regime. The relative independence of the different eyespots thus suggests that their formation involves locally different processes, allowing some independent variation. This result is consistent with artificial selection experiments in *B. anynana* (Beldade *et al.* 2002; Beldade and Brakefield 2003), showing that the independent evolution of eyespots is not strongly constrained by the genetic correlations among eyespots.

A remarkable exception to this global pattern of independence is the tight covariation between the two conditionally-displayed eyespots of *M. telemachus*. In particular, their covariance in FA suggests that specific developmental processes have evolved that jointly affect these two eyespots but not the others. This change in modularity, opposing the conditionally-displayed

eyespots to the always visible eyespots, is likely shaped by the contrasted selective pressures affecting them. Such a change in modularity may result from the adaptive suppression of pleiotropy across groups of traits submitted to different selective pressures (Cheverud, 1984 ; Wagner and Altenberg 1996 ; Breuker *et al.* 2006; Wagner *et al.* 2007; Klingenberg 2014). Studies investigating the adaptive evolution of modularity are still largely lacking (Breuker et al 2006; Klingenberg *et al.* 2010). Our study on the eyespots of *M. telemachus* may thus represent a relevant case where modularity can be tuned by natural selection (Breuker *et al.* 2006). Similar analysis of modularity should be performed in other species harboring heterogeneous morphologies of eyespots, to assess how selection can affect developmental covariations between traits. Experiments are now required to identify (1) the exact selection regime affecting conditionally-displayed eyespots in *M. telemachus* and, (2) the developmental bases underlying the evolution of modularity across *Morpho* species.

References

Allen, C.E., 2008. The "Eyespot Module" and eyespots as modules: development, evolution, and integration of a complex phenotype. J. Exp. Zool. 310B, 179–190.

Allen, J.A., Clarke, B., 1968. Evidence for Apostatic Selection by Wild Passerines. Nature 220, 501–502.

Beldade, P., Brake, P.M., Long, Anthony D., 2002. Contribution of Distal-less to quantitative variation in butterfly eyespots 415, 4.

Beldade, P., Brakefield, P.M., 2002. The genetics and evo–devo of butterfly wing patterns. Nat Rev Genet 3, 442–452.

Beldade, P., Brakefield, P. M. 2003. Concerted evolution and developmental integration in modular butterfly wing patterns. Evolution & Development, 5(2), 169-179.Beldade, P., Monteiro, A., 2021. Eco-evo-devo advances with butterfly eyespots. Current Opinion in Genetics & Development 69, 6–13.

Blandin, P., Purser, B., 2013. Evolution and diversification of Neotropical butterflies: insights from the biogeography and phylogeny of the genus Morpho fabricus, 1807 (Nymphalidae: Morphinae), with a review of the geodynamics of South America 24.

Bond, A.B., 2007. The Evolution of Color Polymorphism: Crypticity, Searching Images, and Apostatic Selection. Annu. Rev. Ecol. Evol. Syst. 38, 489–514.

Bond, A.B., Kamil, A.C., 2006. Spatial heterogeneity, predator cognition, and the evolution of color polymorphism in virtual prey. Proceedings of the National Academy of Sciences 103, 3214–3219.

Bond, A.B., Kamil, A.C., 2002. Visual predators select for crypticity and polymorphism in virtual prey. Nature 415, 609–613.

Bond, A.B., Kamil, A.C., 1998. Apostatic selection by blue jays produces balanced polymorphism in virtual prey. Nature 395, 594–596.

Boonekamp, J.J., Mulder, E., Verhulst, S., 2018. Canalisation in the wild: effects of developmental conditions on physiological traits are inversely linked to their association with fitness. Ecol Lett 21, 857–864.

Brakefield, P. M., 2001. Structure of a character and the evolution of butterfly eyespot patterns. *Journal of Experimental Zoology*, *291*(2), 93-104.

Breuker, C.J., Debat, V., Klingenberg, C.P., 2006. Functional evo-devo. Trends in Ecology & Evolution 21, 488–492.

Breuker, C.J., Gibbs, M., Van Dyck, H., Brakefield, P.M., Klingenberg, C.P., Van Dongen, S., 2007. Integration of wings and their eyespots in the speckled wood butterfly *Pararge aegeria*. J. Exp. Zool. 308B, 454–463.

Chazot, N., Panara, S., Zilbermann, N., Blandin, P., Le Poul, Y., Cornette, R., ... & Debat, V. 2016. Morpho morphometrics: shared ancestry and selection drive the evolution of wing size and shape in Morpho butterflies. *Evolution*, *70*(1), 181-194.

Cheverud, J.M., 1984. Quantitative genetics and developmental constraints on evolution by selection. Journal of Theoretical Biology 110, 155–171.

Clarke, G.M., 1998. The genetic basis of developmental stability. V. Inter- and intra-individual character variation. Heredity 80, 562–567.

Crespi, B.J., Vanderkist, B.A., 1997. Fluctuating asymmetry in vestigial and functional traits of a haplodiploid insect. Heredity 79, 624–630.

Dapporto, L., Hardy, P.B., Dennis, R.L.H., 2019. Evidence for adaptive constraints on size of marginal wing spots in the grayling butterfly, *Hipparchia semele*. Biological Journal of the Linnean Society 126, 131–145.

Debat, V., Chazot, N., Jarosson, S., Blandin, P., Llaurens, V., 2020. What Drives the Diversification of Eyespots in Morpho Butterflies? Disentangling Developmental and Selective Constraints From Neutral Evolution. Front. Ecol. Evol. 8, 112.

Debat, V., David, P., 2001. Mapping phenotypes: canalization, plasticity and developmental stability. Trends in Ecology & Evolution 16, 555–561.

Dell'Aglio, D.D., Troscianko, J., McMillan, W.O., Stevens, M., Jiggins, C.D., 2018. The appearance of mimetic *Heliconius* butterflies to predators and conspecifics. Evolution 72, 2156–2166. https://doi.org/10.1111/evo.13583

Epskamp, S., Cramer, A.O.J., Waldorp, L.J., Schmittmann, V.D., Borsboom, D., 2012. qgraph : Network Visualizations of Relationships in Psychometric Data. J. Stat. Soft. 48.

Emerson, M.J., Schram, F.R., 1990. The Origin of Crustacean Biramous Appendages and the Evolution of Arthropoda. Science 250, 667–669.

Feltz, C.J., Miller, G.E., 1996. An asymptotic test for the equality of coefficients of variation from k populations. Statist. Med. 15, 647–658.

Finkbeiner, S.D., Fishman, D.A., Osorio, D., Briscoe, A.D., 2017. Ultraviolet and yellow reflectance but not fluorescence is important for visual discrimination of conspecifics by *Heliconius erato*. Journal of Experimental Biology jeb.153593.

Forde, B.G., 2009. Is it good noise? The role of developmental instability in the shaping of a root system. Journal of Experimental Botany 60, 3989–4002.

Gabriela Montes-Cartas, C., Padilla, P., Rosell, J.A., Domínguez, C.A., Fornoni, J., Olson, M.E., 2017. Testing the hypothesis that biological modularity is shaped by adaptation: Xylem in the *Bursera simaruba* clade of tropical trees. Evolution & Development 19, 111–123.

Garnier, S., Gidaszewski, N., Charlot, M., Rasplus, J.-Y., Alibert, P., 2006. Hybridization, developmental stability, and functionality of morphological traits in the ground beetle Carabus solieri (Coleoptera, Carabidae). Biological Journal of the Linnean Society 8.

Hall, B.K., 1995. Homology and Embryonic Development. In Evolutionary Biology, 1-30. Springer US, Boston, MA.

Halpin, C.G., Penacchio, O., Lovell, P.G., Cuthill, I.C., Harris, J.M., Skelhorn, J., Rowe, C., 2020. Pattern contrast influences wariness in naïve predators towards aposematic patterns. Sci Rep 10, 9246.

Huq, M., Bhardwaj, S., Monteiro, A., 2019. Male *Bicyclus anynana* Butterflies Choose Females on the Basis of Their Ventral UV-Reflective Eyespot Centers. Journal of Insect Science 19.

Inglis, I.R., Huson, L.W., Marshall, M.B., Neville, P.A., 2010. The Feeding Behaviour of Starlings (Sturnus vulgaris) in the Presence of 'Eyes.' Zeitschrift für Tierpsychologie 62, 181–208.

Kirschner, M., & Gerhart, J. (1998). Evolvability. *Proceedings of the National Academy of Sciences*, *95*(15), 8420-8427.

Klingenberg, C.P., 2003. Developmental instability as a research tool: using patterns of fluctuating asymmetry to infer the developmental origins of morphological integration. In Developmental Stability: Causes and Consequences, 427–442. Oxford University Press.

Klingenberg, C.P., Monteiro, L.R., 2005. Distances and Directions in Multidimensional Shape Spaces: Implications for Morphometric Applications. Systematic Biology 54, 678–688.

Klingenberg, C.P., 2008. Morphological Integration and Developmental Modularity. Annu. Rev. Ecol. Evol. Syst. 39, 115–132.

Klingenberg, C. P. 2014. Studying morphological integration and modularity at multiple levels: concepts and analysis. Philosophical Transactions of the Royal Society B: Biological Sciences, 369(1649), 20130249.

Klingenberg, C. P., Debat, V., & Roff, D. A., 2010. Quantitative genetics of shape in cricket wings: developmental integration in a functional structure. Evolution: International Journal of Organic Evolution, 64(10), 2935-2951.

Kodandaramaiah, U., 2011. The evolutionary significance of butterfly eyespots. Behavioral Ecology 22, 1264–1271.

Lahti, D. C., Johnson, N. A., Ajie, B. C., Otto, S. P., Hendry, A. P., Blumstein, D. T., ... & Foster, S. A., 2009. Relaxed selection in the wild. *Trends in ecology & evolution*, *24*(9), 487-496.

Leamy, L.J., Klingenberg, C.P., 2005. The Genetics and Evolution of Fluctuating Asymmetry. Annu. Rev. Ecol. Evol. Syst. 36, 1–21.

Lyytinen, A., Brakefield, P.M., Lindström, L., Mappes, J., 2004. Does predation maintain eyespot plasticity in *Bicyclus anynana*? Proc. R. Soc. Lond. B 271, 279–283.

Maia, R., Gruson, H., Endler, J.A., White, T.E., 2019. PAVO 2: New tools for the spectral and spatial analysis of colour in R. Methods Ecol Evol 10, 1097–1107.

Marwick, B., Krishnamoorthy, K., 2019. cvequality: Tests for the Equality of Coefficients of Variation from Multiple Groups.

519 Meijering, E.H.W., Niessen, W.J., Viergever, M.A., 2001. Quantitative evaluation of
520 convolution-based methods for medical image interpolation. Medical Image Analysis 5,
521 111–126.
522 Melo, D., Marroig, G., 2015. Directional selection can drive the evolution of modularity in
523 complex traits. Proc. Natl. Acad. Sci. U.S.A. 112, 470–475.
524 Monteiro, A., 2015. Origin, Development, and Evolution of Butterfly Eyespots. Annu. Rev.
525 Entomol. 60, 253–271.
526 Monteiro, A., 2008. Alternative models for the evolution of eyespots and of serial homology on
527 lepidopteran wings. Bioessays 30, 358–366.
528 Monteiro, A., Brakefield, P.M., French, V., 1997. Butterfly eyespots: the genetics and
529 development of the color rings. Evolution 51, 1207–1216.
530 Monteiro, A.F., Brakefield, P.M., French, V., 1994. The evolutionary genetics and
531 developmental basis of wing pattern variation in the butterfly Bicyclus anynana.
532 Evolution 48, 1147–1157.
533 Olofsson, M., Vallin, A., Jakobsson, S., Wiklund, C., 2010. Marginal Eyespots on Butterfly
534 Wings Deflect Bird Attacks Under Low Light Intensities with UV Wavelengths. PLoS
535 ONE 5, e10798.
536 Olsson, P., Lind, O., Kelber, A., 2018. Chromatic and achromatic vision: parameter choice and
537 limitations for reliable model predictions. Behavioral Ecology 29, 273–282.
538 Osorio, D., Miklósi, A., Gonda, Zs., 1999. Visual Ecology and Perception of Coloration Patterns
539 by Domestic Chicks. Evolutionary Ecology 13, 673–689.
540 Palmer, A.R., 1994. Fluctuating asymmetry analyses: a primer, in: Markow, T.A. (Ed.),
541 Developmental Instability: Its Origins and Evolutionary Implications, Contemporary
542 Issues in Genetics and Evolution. Springer Netherlands, Dordrecht, pp. 335–364.
543 Palmer, A.R., Strobeck, C., 1986. Fluctuating Asymmetry: Measurement, Analysis, Patterns.
544 Annual Review of Ecology and Systematics 17, 391–421.
545 Pavlicev, M., & Wagner, G. P. (2012). A model of developmental evolution: selection,
546 pleiotropy and compensation. *Trends in Ecology & Evolution*, *27*(6), 316-322.
547 Pélabon, C., Hansen, T.F., Carter, A.J.R., Houle, D., 2010. Evolution of variation and variability
548 under fluctuating, stabilizing, and disruptive selection. Evolution 64, 1912–1925.
549 Prudic, K.L., Skemp, A.K., Papaj, D.R., 2007. Aposematic coloration, luminance contrast, and
550 the benefits of conspicuousness. Behavioral Ecology 18, 41–46.

551 Prudic, K.L., Jeon, C., Cao, H., Monteiro, A., 2011. Developmental Plasticity in Sexual Roles
552 of Butterfly Species Drives Mutual Sexual Ornamentation. Science 331, 73–75.
553 Prudic, K.L., Stoehr, A.M., Wasik, B.R., Monteiro, A., 2015. Eyespots deflect predator attack
554 increasing fitness and promoting the evolution of phenotypic plasticity. Proc. R. Soc. B.
555 282, 20141531.
556 Robertson, K.A., Monteiro, A., 2005. Female *Bicyclus anynana* butterflies choose males on the
557 basis of their dorsal UV-reflective eyespot pupils. Proc. R. Soc. B. 272, 1541–1546.
558 Schlosser, G., & Wagner, G. P. (Eds.). 2004. *Modularity in development and evolution*.
559 University of Chicago Press.
560 Schluter, D., 1996. Adaptive radiation along genetic lines of least resistance. Evolution 50,
561 1766–1774.
562 Schmalhausen, I. I., 1949. Factors of evolution: the theory of stabilizing selection. *University*
563 *of Chicago Press*, 1987.
564 Sinervo, B., & Svensson, E., 2002. Correlational selection and the evolution of genomic
565 architecture. *Heredity*, *89*(5), 329-338.
566 Stearns, S.C., Kaiser, M., Kawecki, T.J., 1995. The differential genetic and environmental
567 canalization of fitness components in Drosophila melanogaster. J Evolution Biol 8, 539–
568 557.
569 Stevens, M., 2005. The role of eyespots as anti-predator mechanisms, principally demonstrated
570 in the Lepidoptera. Biological Reviews 80, 573–588.
571 Suzuki, R., Terada, Y., Shimodaira, H., 2019. pvclust: Hierarchical Clustering with P-Values
572 via Multiscale Bootstrap Resampling version 2.2-0 from CRAN [WWW Document].
573 URL https://rdrr.io/cran/pvclust/ (accessed 12.15.21).
574 Tague, R. G., 1997. Variability of a vestigial structure: first metacarpal in *Colobus guereza* and
575 *Ateles geoffroyi*. *Evolution*, *51*(2), 595-605.
576 Tague, R. G., 2002. Variability of metapodials in primates with rudimentary digits: *Ateles*
577 *geoffroyi*, *Colobus guereza*, and *Perodicticus potto*. *American Journal of Physical*
578 *Anthropology 117*(3), 195-208.
579 Tague, R. G., 2020. Rudimentary,“functionless” first metapodials of *Canis latrans*: Variation
580 and association in length with longer, functional metapodials. *Evolution*, *74*(11), 2465-
581 2482.
582 Théry, M., Debut, M., Gomez, D., Casas, J., 2004. Specific color sensitivities of prey and
583 predator explain camouflage in different visual systems. Behavioral Ecology 16, 25–29.

Ursprung, H., Nöthiger, R. (Eds.), 1972. The Biology of Imaginal Disks, Results and Problems in Cell Differentiation. Springer Berlin Heidelberg, Berlin, Heidelberg.

Van Valen, L., 1994. Serial homology: the crests and cusps of mammalian teeth. Acta Palaeontologica Polonica 38, 145–158.

Wagner, G.P., Altenberg, L., 1996. Perspective: Complex adaptations and the evolution of evolvability. Evolution 50, 967–976.

Wagner, G.P., Pavlicev, M., Cheverud, J.M., 2007. The road to modularity. Nat Rev Genet 8, 921–931.

Ward, J.H., 1963. Hierarchical Grouping to Optimize an Objective Function. Journal of the American Statistical Association 236–244.

Young, N.M., Hallgrimsson, B., 2005. Serial homology and the evolution of Mammalian limb covariation structure. Evol 59, 2691.

Zelditch, M.L., Wood, A.R., Bonett, R.M., Swiderski, D.L., 2008. Modularity of the rodent mandible: Integrating bones, muscles, and teeth: Modularity of the rodent mandible. Evolution & Development 10, 756–768.

Figures legends

Figure 1: Eyespots observed on the ventral sides of the wings in *Morpho telemachus* and *Morpho helenor*. (A) Picture of *M. telemachus* taken in resting position, showing the always-visible eyespots. Photo credit: Peter Møllmann. (B) Position and numbering of the measured eyespots. Eyespots E3 and E4, figured in dark and light orange, are conditionally-displayed in *M. telemachus* (they are usually hidden by the hindwing at rest), and always exposed in *M. helenor*. The other eyespots are figured in grey. Left - *M. telemachus*: Right - *M. helenor*. (C) The four measurements taken on each eyespot (length and width of the yellow and black rings, respectively noted L_y, W_y, L_b and W_b).

Figure 2: Sizes, shapes and colors of eyespots, revealing contrasted levels of conspicuousness in *M. telemachus and M. helenor*. Eyespots E3 and E4 (conditionally-displayed in *M. telemachus*) are figured in orange. Circles: *M. telemachu*s; triangles: *M. helenor*. **A**: Eyespots sizes. The four measurements are similarly different across eyespots, so only L_y is displayed. Boxplots indicate mean and standard deviation. Significant differences between eyespots are shown using different letters (a, b, c) – results for *M. telemachus* are

displayed in full letters (above) and results for *M. helenor* are displayed in italic letters (below). **B**: Deviation from roundness of *M. telemachus* eyespots yellow rings (assessed by L_y /W_y ratio). **C**: Achromatic contrast (JND) between the yellow and the black rings of each eyespot. Results are similar across the 2 vision models, so only the UV-model results are displayed (see Figure S1 for chromatic contrasts).

Figure 3: High levels of shape variability in *M. telemachus* always-visible eyespots suggest a relaxed selection. Inter-individual variation (top) and fluctuating asymmetry (bottom) of eyespots yellow ring shape (L_y/W_y). For each species, significant differences between eyespots are shown using different letters (a, b, c; a letter pools non-significantly different traits). Left: *M. telemachus* (n = 370); right: *M. helenor* (n = 31). The relatively low variability of E3 and E4 is comparable to that observed in most *M. helenor* eyespots, suggesting a similar stabilizing selection. The high variability of *M. telemachus* always-visible eyespots in turn suggests a relaxed or apostatic selection.

Figure 4: Contrasted patterns of modularity observed in *M. telemachus* and *M. helenor*. as assessed by correlation matrices of linear parameters (L_y, W_y, L_b, W_b) of the 7 different eyespots. Top: *M. helenor* (n = 31); Bottom: *M. telemachus* (n = 370). Left: modularity patterns inferred from individual variation; Right: modularity patterns inferred from FA. Nodes represent the 4 measured variables and the edges represent the statistically significant correlations. Line thickness is proportional to the correlation. The blue ellipse shows the module regrouping E3 and E4 detected by the hierarchical clustering in *M. telemachus*.

Figure 5: Hierarchical clustering based on the FA and inter-individual correlation matrices of linear parameters (L_y, W_y, L_b, W_b) of the 7 different eyespots. *M. telemachus* (n = 370) is shown on the second row and *M. helenor* (n = 31) on the first row. Left: Hierarchical clustering based on the inter-individual correlation matrices. Right: Hierarchical clustering based on FA correlation matrices. Hierarchical clustering exploring the networks modularity. The height of the nodes indicates the distance between two observations (here we used correlation matrix as distance matrix, so the higher the height, the less correlated are two traits). A node market with a blue circle indicate that the associated cluster is significant. The cluster associating the conditionally-displayed eyespots E3 and E4 in *M. telemachus* is the only cluster whose intra-eyespot modularity is overcome by inter-eyespots modularity.

Appendices

Figure S1: Chromatic contrasts (JND) between the yellow ring and the black ring of eyespots measured in *M. telemachu*s (n = 10; circles) and *M. helenor* (n = 10; triangles). The 2 vision models are displayed: UV-sensitive birds (left) and Violet-sensitive birds (right).

Figure S2: Fluctuating asymmetry of eyespots linear parameters, respectively length and width of the yellow ring (L_y and W_y) and length and width of the black ring (L_b and W_b) of each eyespot (E1, E3, E4, E5, E7, E8 and E9), measured in the *M. telemachus* sample (n = 370) and *M. helenor* (n = 31). Significant differences between eyespots are shown using different letters (a, b, c) – results for *M. telemachus* are displayed in full letters (above) and results for *M. helenor* are displayed in italic letters (below).

Figure S3: Inter-individual variation of eyespots linear parameters, respectively length and width of the yellow ring (L_y and W_y) and length and width of the black ring (L_b and W_b) of each eyespot (E1, E3, E4, E5, E7, E8 and E9), measured in the *M. telemachus* sample (n = 370) and *M. helenor* (n = 31).

Table S1: Pairwise comparisons of size differences among *M. telemachus* eyespots (L_y measures), using Welch's tests, and accounting for multiple comparisons using Holm-Bonferroni correction. The sample size for all tests is 370.

Table S2: Pairwise comparisons of the yellow ring shape among *M. telemachus* eyespots (R_y measures), using Welch's tests and accounting for multiple testing by using Holm-Bonferroni correction. The sample size for all tests is 370.

Table S3: Summary of the measured correlations between eyespots of *M. telemachus* and *M. helenor* – especially between conditionally-displayed (E3-E4) and always-visible (AV) eyespots. Table indicate mean and standard deviation.


A

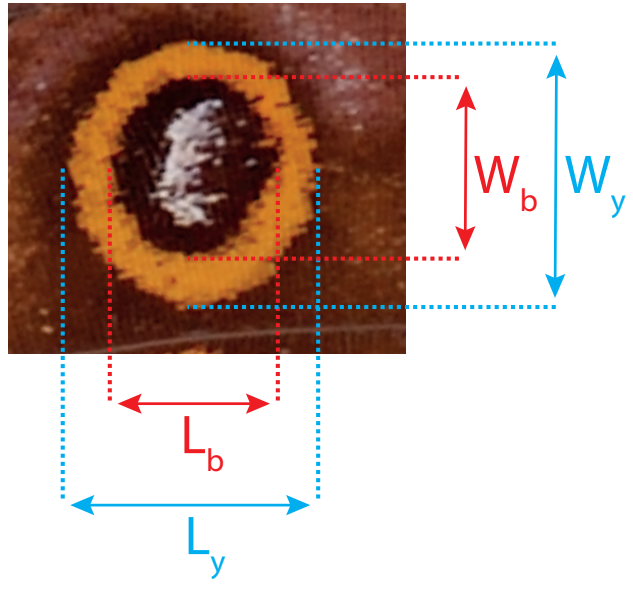
C
W b
W y
L b
L y

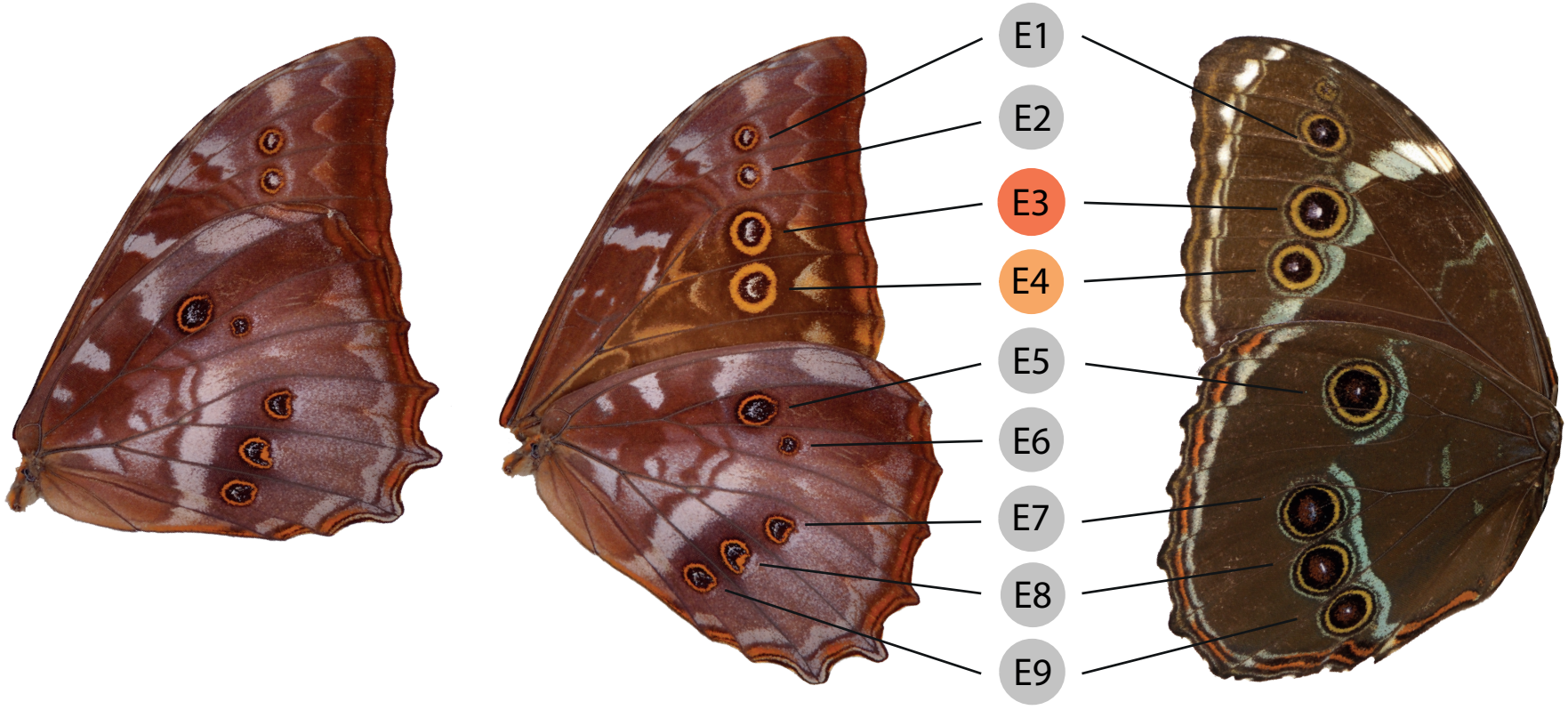
B
E1
E2
E3
E4
E5
E6
E7
E8
E9

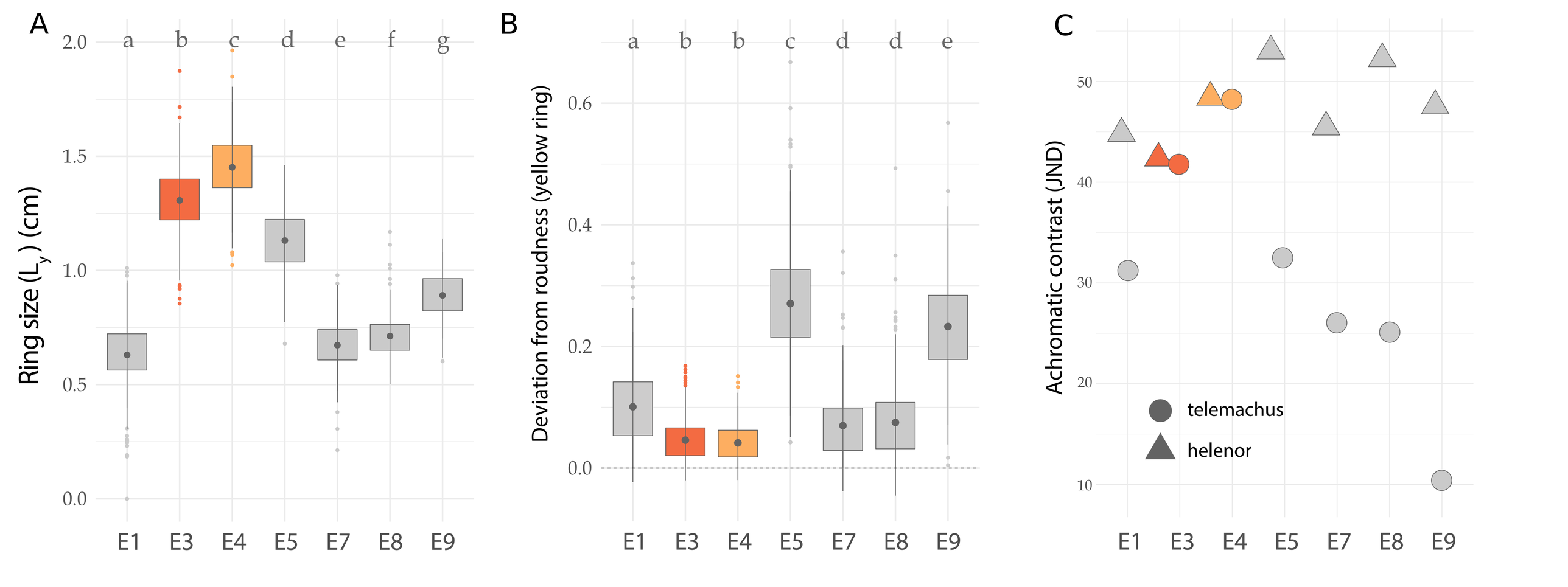
A
B
C
Ring size (L_y) (cm)
Deviation from roudness (yellow ring)
Achromatic contrast (JND)
a b c d e f g
a b b c d d e
E1 E3 E4 E5 E7 E8 E9
telemachus
helenor

M. telemachus

M. helenor

Inter-individual variation

0.015
0.010
0.005
0.000

a b b c c c d

ab c c ac ab ab b

E1 E3 E4 E5 E7 E8 E9

Fluctuating Asymmetry

0.05
0.04
0.03
0.02
0.01
0.00

a b b c a a d

a c c c c c a

E1 E3 E4 E5 E7 E8 E9

Individual variation

Fluctuating asymmetry

M. helenor

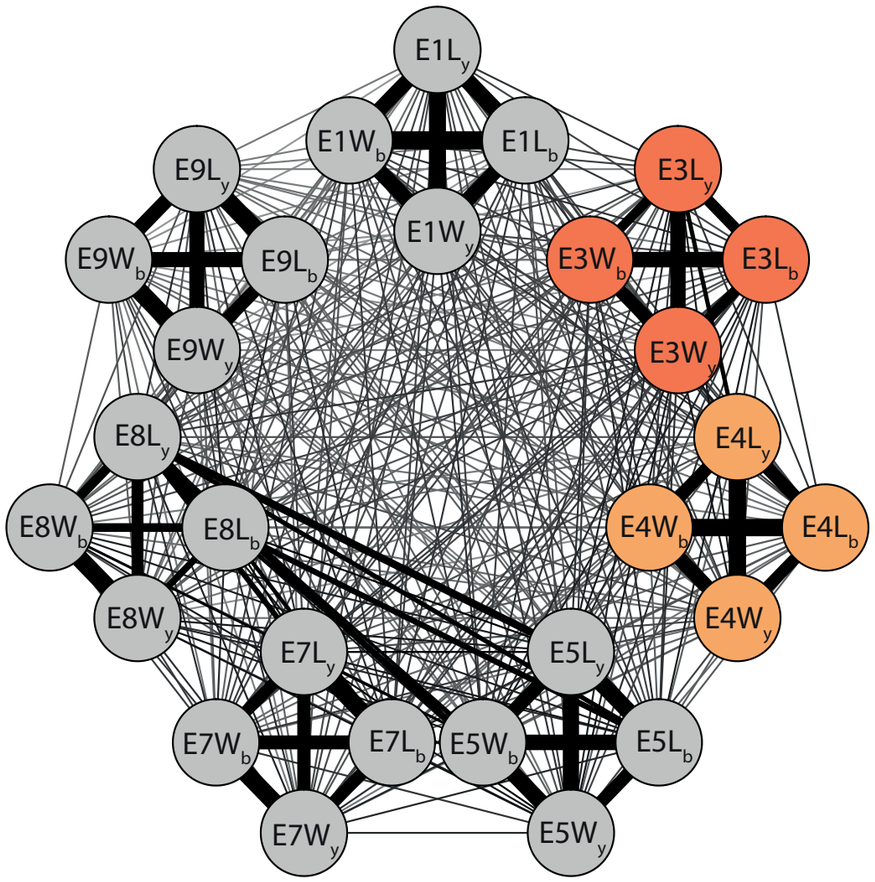

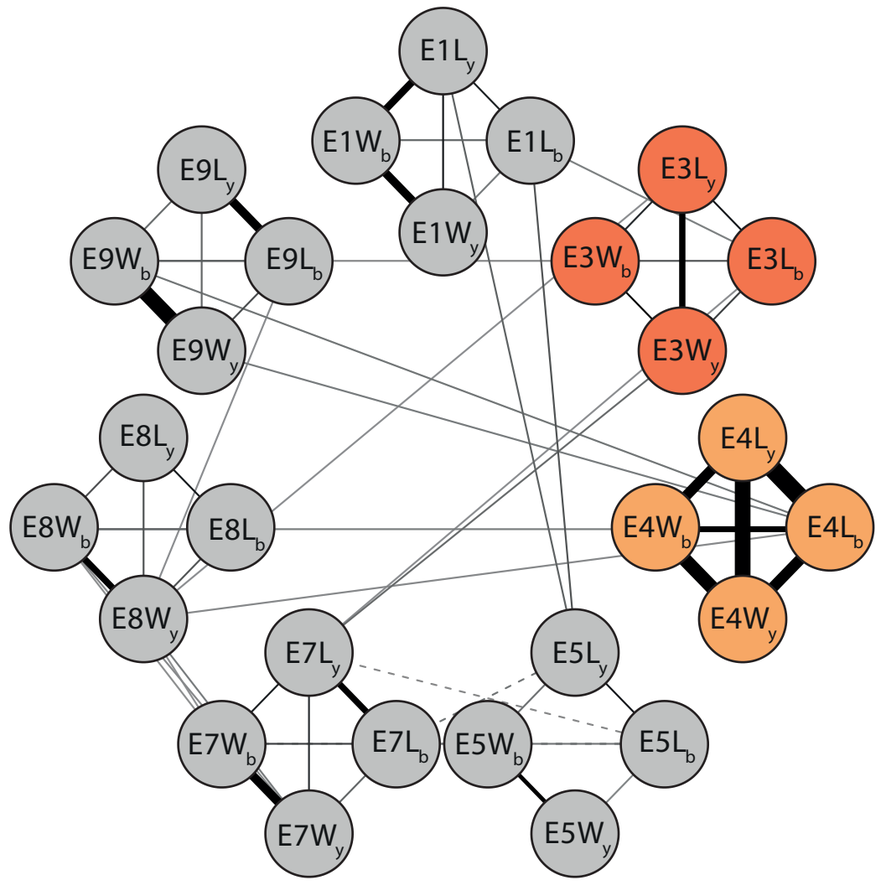

Correlation

0.2
0.4
0.6
0.8
1

M. telemachus

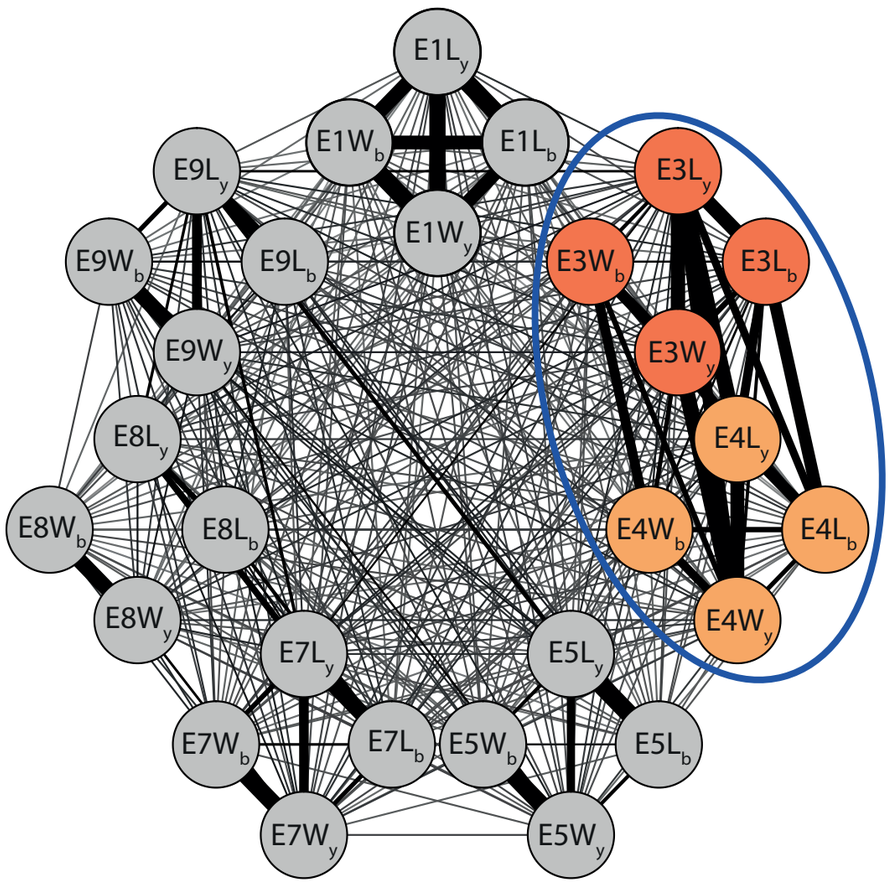

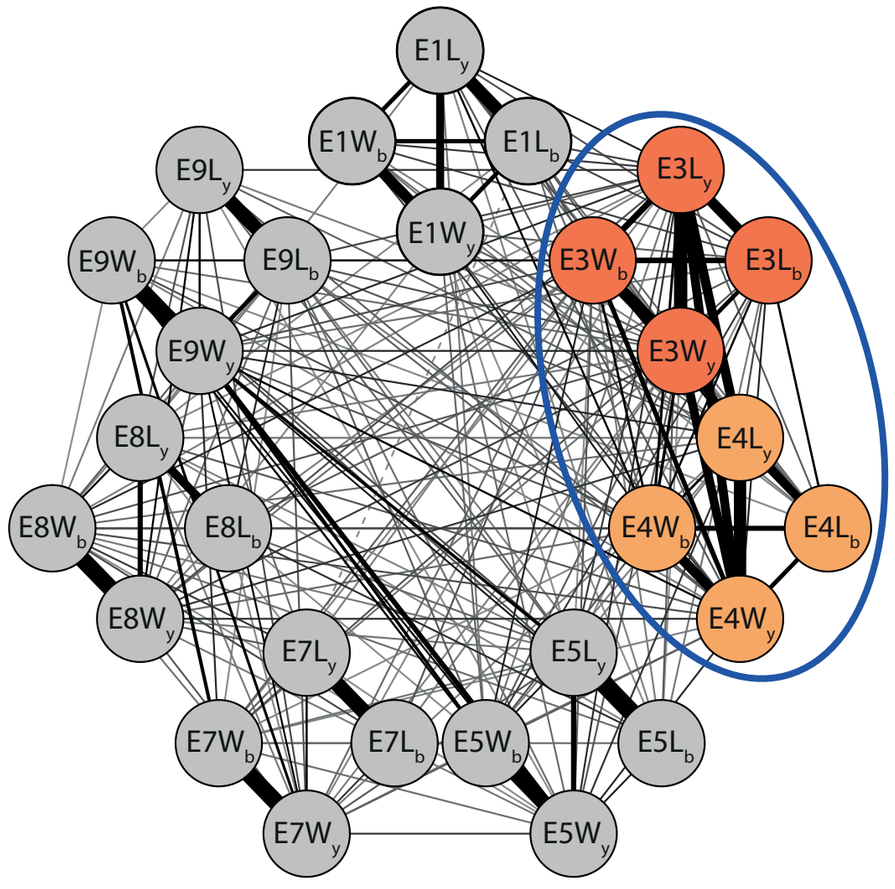

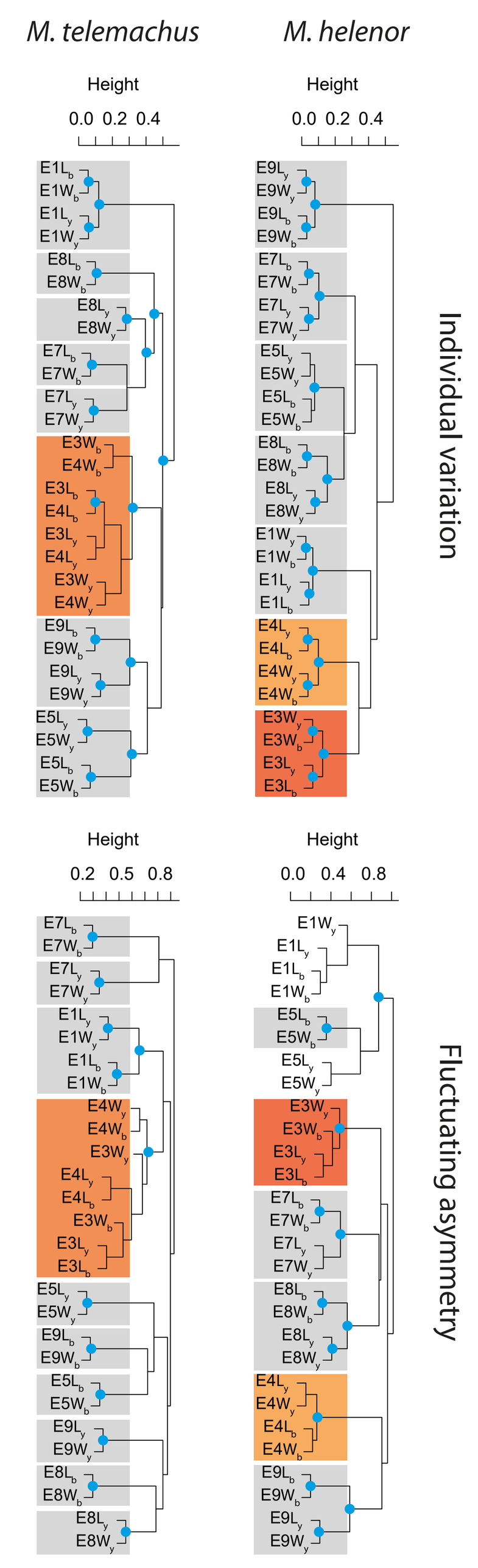
M. telemachus
M. helenor
Height
0.0 0.2 0.4
E1L_b
E1W_b
E1L_y
E1W_y
E8L_b
E8W_b
E8L_y
E8W_y
E7L_b
E7W_b
E7L_y
E7W_y
E3W_b
E4W_b
E3L_b
E4L_b
E3L_y
E4L_y
E3W_y
E4W_y
E9L_b
E9W_b
E9L_y
E9W_y
E5L_y
E5W_y
E5L_b
E5W_b
E9L_y
E9W_y
E7L_b
E7W_b
E7L_y
E7W_y
E5L_y
E5W_y
E5L_b
E5W_b
E8L_b
E8W_b
E8L_y
E8W_y
E1W_y
E1W_b
E1L_y
E1L_b
E4L_y
E4L_b
E4W_y
E4W_b
E3W_y
E3W_b
E3L_y
E3L_b
Individual variation
Height
0.2 0.5 0.8
0.0 0.4 0.8
E7L_b
E7W_b
E7L_y
E7W_y
E1L_y
E1W_y
E1L_b
E1W_b
E4W_y
E4W_b
E3W_y
E4L_y
E4L_b
E3W_b
E3L_y
E3L_b
E5L_y
E5W_y
E9L_b
E9W_b
E5L_b
E5W_b
E9L_y
E9W_y
E8L_b
E8W_b
E8L_y
E8W_y
E1W_y
E1L_y
E1L_b
E1W_b
E5L_b
E5W_b
E5L_y
E5W_y
E3W_y
E3W_b
E3L_y
E3L_b
E7L_b
E7W_b
E7L_y
E7W_y
E8L_b
E8W_b
E8L_y
E8W_y
E4L_y
E4W_y
E4L_b
E4W_b
E9L_b
E9W_b
E9L_y
E9W_y
Fluctuating asymmetry